Bioresource Technology 407 (2024) 131064

Contents lists available at ScienceDirect

Bioresource Technology

journal homepage: www.elsevier.com/locate/biortech

Modelling anaerobic sulfide removal by sulfide shuttling bacteria

Joris Bergman [a,c], Annemerel R. Mol [b], Annemiek ter Heijne [b,*], Karel J. Keesman [a,c,*], Rikke Linssen [b]

[a] Wetsus, European Centre of Excellence for Sustainable Water Technology, Oostergoweg 9, 8911 MA Leeuwarden, the Netherlands
[b] Environmental Technology, Wageningen University, P.O. Box 17, Bornse Weilanden 9, 6708 WG, the Netherlands
[c] Mathematical and Statistical Methods (Biometris), Wageningen University, P.O. Box 16, 6700 AA Wageningen, the Netherlands

HIGHLIGHTS

- Anaerobic sulfide removal by sulfide oxidizing bacteria increases with pH.
- Sulfide removal can be explained by ensuing fast chemical and slow enzymatic steps.
- A new two-stage model integrates a chemical and a biological product-limited step.
- The new model outperforms two other models in multiple datasets.
- Biomass composition determines the initial (fast) sulfide removal rate.

GRAPHICAL ABSTRACT

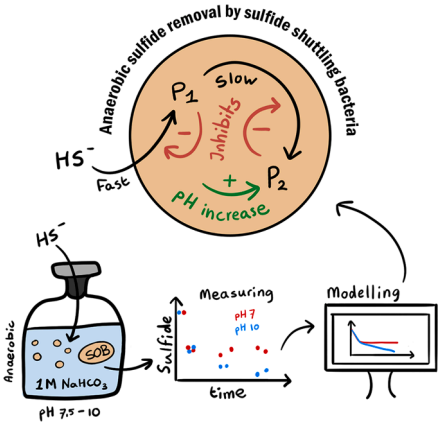

ARTICLE INFO

Keywords:
Biodesulfurization
Charge storage
Kinetics
Sulfide oxidizing bacteria
Parameter estimation
Gas treatment

ABSTRACT

Sulfide oxidizing bacteria are used in industrial biodesulfurization processes to convert sulfide to sulfur. These bacteria can spatially separate sulfide removal from terminal electron transfer, thereby acting as sulfide shuttles. The mechanisms underlying sulfide shuttling are not yet clear. In this work, newly obtained sulfide removal data were used to develop a new model for anaerobic sulfide removal and this model was shown to be an improvement over two previously published models. The new model describes a fast chemical step and a consecutive slow enzymatic step. The improved model includes the effect of pH, with higher total sulfide removal at increasing pH, as well as partial sulfide removal at higher sulfide concentrations. The two-stage model is supported by recent developments in anaerobic sulfide removal research and contributes to a better understanding of the underlying mechanisms. The model is a step toward accurately modelling anaerobic sulfide removal in industrial systems.

* Corresponding authors.
E-mail addresses: annemiek.terheijne@wur.nl (A. ter Heijne), karel.keesman@wur.nl (K.J. Keesman).

https://doi.org/10.1016/j.biortech.2024.131064
Received 7 May 2024; Received in revised form 2 July 2024; Accepted 2 July 2024
Available online 2 July 2024

1. Introduction

Hydrogen sulfide (H_2S), a toxic and odorous gas, is present in several industrial waste streams (Feilberg et al., 2017; Singh and Chandra, 2019). Biodesulfurization under haloalkaline conditions (pH 8–9, [Na^+] 1–1.5 M) is an environmentally friendly remediation process for gas streams containing H_2S. The process makes use of the natural ability of haloalkaline sulfide oxidizing bacteria (SOB) to convert sulfide to stable and harmless sulfur particles (Janssen et al., 2009). Sulfide is first absorbed in an absorber column and then converted by SOB to sulfur in an aerated reactor. This sulfur is recovered in a settler or a decanter-centrifuge. Since its development, the process has seen numerous improvements, among them the addition of an anaerobic reactor between the absorber and the aerated reactor (de Rink et al., 2021). In this anaerobic reactor, lower sulfide concentrations are measured than expected based on the sulfide loading rate and liquid flow rate (de Rink et al., 2021). In batch experiments, full sulfide removal could be achieved (Linssen et al., 2023). Nevertheless, oxygen is still consumed in the aerated reactor. Therefore, bacteria act as sulfide shuttles: removing sulfide in one reactor and consuming oxygen in the other. Recent investigations on sulfide shuttling have yet to give conclusive answers on its precise mechanisms (Linssen et al., 2024, 2023).

Polysulfides have long been hypothesized to play a role in anaerobic sulfide removal (de Rink et al., 2021; Linssen et al., 2024, 2023). Rotating disc electrode experiments revealed that SOB form polysulfides that stay sorbed to the cell (Linssen et al., 2024). These polysulfides can be formed through the reaction of HS^- with elemental sulfur found in the periplasm of the SOB. Inorganic polysulfides (S_x^{2-}) are subject to a chemical equilibrium with HS^- and consequently cannot fully account for the removal observed in Linssen et al. (2023). This means that after the initial formation, further reactions must take place and anaerobic sulfide removal is a multi-step process.

Polysulfides are more stable at higher pH values and, in the continuous biodesulfurization process, higher sulfide removal was found at higher pH values (de Rink et al., 2021). However, the effect of pH had not been quantified in Linssen et al. (2023) and thus needs further investigation. To further investigate anaerobic sulfide removal by SOB, batch sulfide removal experiments were performed varying different conditions, such as pH and SOB community composition.

To the authors' knowledge, the only available models for anaerobic sulfide removal are the models published in Linssen et. al. (Linssen et al., 2023). The model presented in Linssen et al. (2023) (Model 1, Fig. 1) combines parallel passive chemical and active biological removal steps, with the biological process contributing to over 95 % of the total sulfide removal. Additionally, an alternative model that described a single, product limited, biological removal step (Model 2) was described in the SI of Linssen et al. (2023). Both models adequately described the data published in Linssen et al. (2023) but performed poorly on the data gathered in the current study, which had been gathered using a different biomass consortium (Fig. 2 A-D). In this study, a two-stage model (Model 3) is proposed and fit to data gathered in both this study and Linssen et al. (2023). A systematic approach to parameter estimation is presented and the model performance is compared to Models 1 and 2.

2. Materials and methods

2.1. Sulfide removal experiments

Reactor effluent containing SOB, sulfur particles and sodium (bi) carbonate buffer, originated from a bench-scale biodesulfurization setup as described in Kiragosyan et al. (2020). Sulfide removal experiments were performed using the method described in Linssen et al. (2023). Biomass concentration is expressed as total suspended nitrogen (LCK138, Hach, The Netherlands). Biomass was isolated from the reactor effluent by centrifugation and resuspending in 1 M (bi)carbonate buffer at 200–400 mgN L^{-1}. In batch bottles, biomass was diluted to 11 mgN L^{-1} with 1 M sodium (bi)carbonate buffers at pH of 7.5, 8, 9, and 10, and made anoxic by stripping with nitrogen gas for 10 min. Then, a dissolved sulfide stock solution was added to achieve an initial $[HS^-]$ of 0.35 mM. For 30 min, samples were taken periodically and the sulfide concentration was determined by spectrophotometric assay (LCK653, Hach, The Netherlands).

2.2. Microbial community analysis

To be able to compare the microbial community used in this study to the one used in Linssen et al. (2023). DNA extraction was done using DNeazy power soil pro kit (Qiagen, Germany). Further amplification of DNA using the V3-V4 of 16 s rDNA, as well as DNA analysis was performed as described in De Smit et al. (2019) using SILVA reference database to pick operational taxonomic units and classify the sequences.

2.3. Sulfide removal models

In this work, three models as described in the introduction and shown in Fig. 1 are compared.

Model 3 is based on two consecutive, product limited chemical and biological steps. The proposed reaction structure for Model 3 assumes that HS^- reacts to an intermediate product P_1 which then reacts to form P_2. In this model, P_1 is the product of the initial adsorption step described in Linssen et al. (2024), in which sulfide enters the periplasmic space and forms polysulfides, and P_2 represents a (collection of) more stable reaction product(s).

The initial reaction rate r_1 to P_1(mM) is fast and after reaching a critical product concentration $K_{i,1}$ (mM), $r_1 = 0$. Therefore, the rate-limiting step becomes the conversion of P_1 to P_2, with reaction rate r_2. This continues until the SOB is unable to take on more charge.

The rates for the two reactions are given by Eqs. (1) and (2), and the mass balances for the three compounds are given by Eqs. 3–5.

$$r_1 = k_1[HS^-]\left(1 - \frac{[P_1]}{K_{i,1}}\right)X_b \tag{1}$$

$$r_2 = v_{max}\frac{[P_1]}{[P_1] + K_m}\exp\left(-\frac{[P_2]}{K_{i,2}}\right)X_b \tag{2}$$

$$\frac{d[HS^-]}{dt} = -r_1 \tag{3}$$

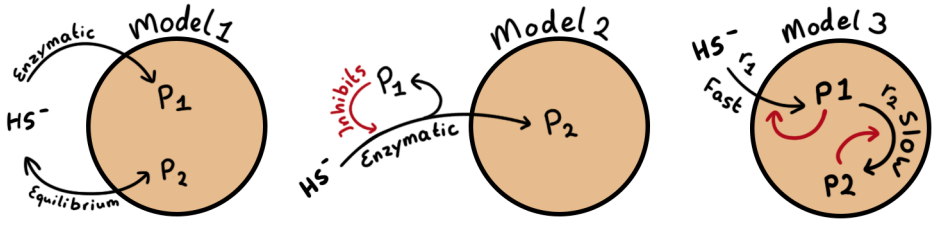

Fig. 1. Visual representation of sulfide removal models discussed in this work. P_1 and P_2 depict different unknown products. Red arrows depict the inhibitory effect of products on conversion rates. The circles of the three models symbolize bacterial cells, with the line being the outer membrane and the brown inside the periplasm.

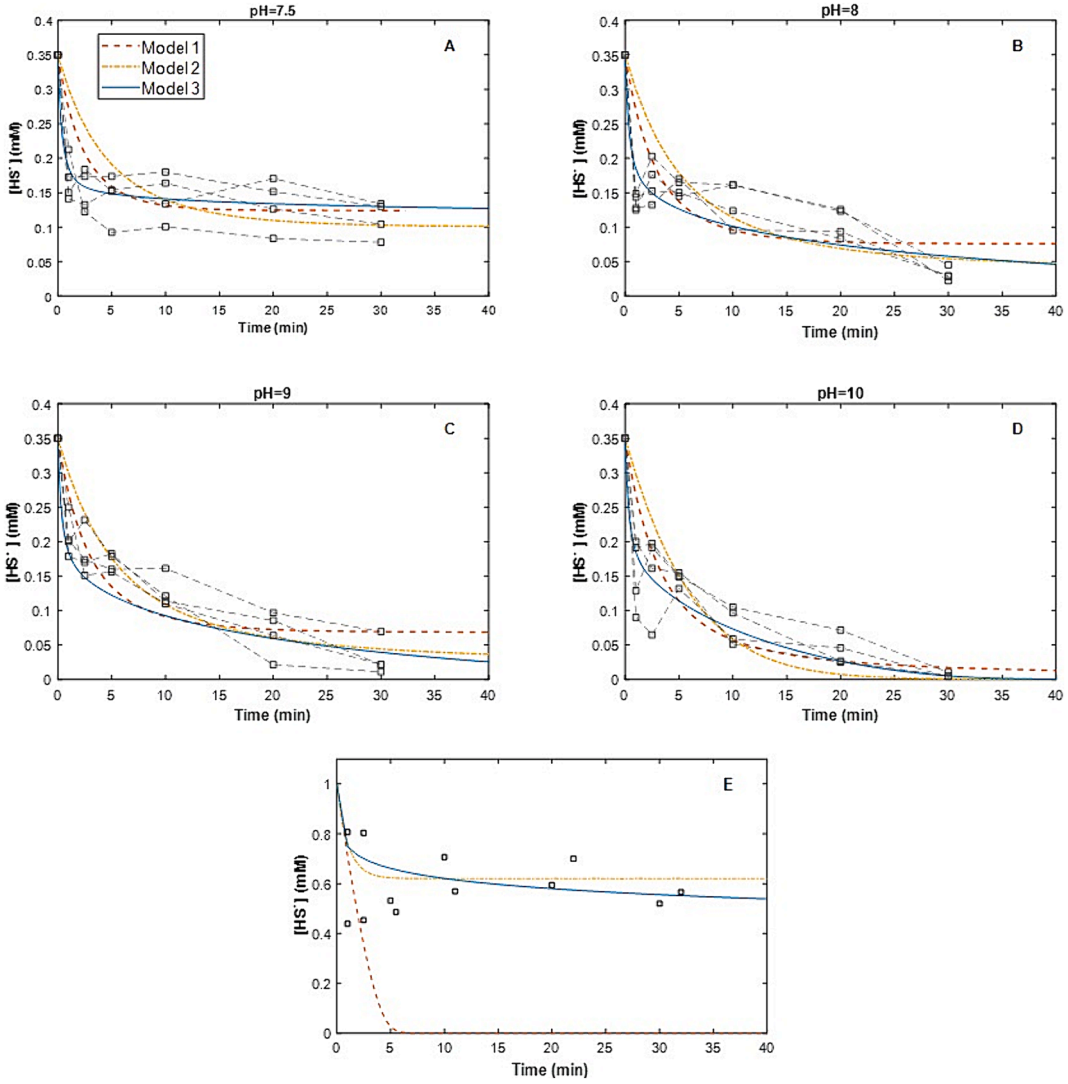

Fig. 2. A-D): Sulfide concentration after dosing 0.35 mM sulfide to 11 mgN L^{-1} sulfide shuttling bacteria under anaerobic conditions at pH 7.5 (A), 8 (B), 9 (C), and 10 (D). Shown are the trajectories of the individual technical replicates (n = 4), with each square representing a single measured value, and the fit of Models 1,2 and 3. E) Sulfide removal data obtained at pH 8.5, after dosing 1 mM sulfide to 24 mgN L^{-1} biomass (different composition than this work) (Linssen et al. 2023) and model fit of Models 1,2 and 3.

$$\frac{d[P_1]}{dt} = r_1 - r_2 \tag{4}$$

$$\frac{d[P_2]}{dt} = r_2 \tag{5}$$

In which k_1 is the kinetic rate constant in s^{-1} L mgN^{-1}, ν_{max} the maximal rate in mM s^{-1} L mgN^{-1},$[P_i]$, for $i = 1, 2$, the concentration of the products in mM, $K_{i,j}$, for $j = 1,2$, the inhibition constant in mM, K_m the Monod constant in mM and X_b the biomass concentration in mgN L^{-1}. The rate r_1 is approximated by a first-order kinetic term, due to its rapid rate and the fact that its abrupt transition to a regime dominated by r_2 is caused by product inhibition when $[P_1] = K_{i,1}$. For the inhibition, two terms are used. The Han-Levenspiel term for non-competitive inhibition (Muloiwa et al., 2020) is used for r_1. This represents a chemical equilibrium being achieved in the periplasmic space, as at equilibrium no net reaction should take place.

An Aiba-Edwards inhibition term (Muloiwa et al., 2020) is used to describe the product inhibition term for r_2. It is assumed that, since the environment is anoxic, the SOB have no access to an external electron acceptor. Therefore, as the SOB produce more P_2, they become more reduced. Consequently, the availability of internal electron storage decreases gradually leading to increasing inhibition.

3. Results and discussion

3.1. Parameter estimation

In Eq. 1–2 five unknowns (k_1, ν_{max}, K_m, $K_{i,1}$ and $K_{i,2}$) had to be estimated from only one measured output, $[HS^-]$. The parameter K_m typically shows strong cross-correlation with ν_{max} in parameter estimation problems (Holmberg and Ranta, 1982). Furthermore, accurate estimation of K_m would require multiple measurements of P_1. Instead, K_m was fixed at its nominal value of 0.15 mM taken from Model 2 (Linssen et al., 2023) in order to have a correct order of magnitude estimation.

Simultaneous estimation of the four remaining parameters using a least-squares method described in Linssen et al. (2023) revealed large uncertainties in specific parameter combinations. Therefore, a dynamic parametric sensitivity analysis was carried out using the method described in Klok (2015). From this analysis, it was found that $[HS^-]$ was most sensitive to ν_{max} and $K_{i,2}$ (see supplementary information). Furthermore, $[HS^-]$ was only sensitive to k_1 on the interval$t = 0$ to $t = 5$

which is right after the injection of sulfide. The sensitivity to $K_{i,1}$ reached its maximum around t = 1, when the inclination of the graphs in Fig. A-D decreases. The estimate of $K_{i,1}$ was therefore determined based on the amount of HS^- removed at that point. The estimate of k_1 determined from the initial $[HS^-]$ between $t = 0$ and $t = 1$. Since the initial part of the graph is approximately linear, it is assumed that $[P_1] \approx \frac{1}{2}K_{i,1}$, because at $t = 0, P_1 = 0$ and at $t = 1, P_1 = K_{i,1}$. Substituting this value into Eq. (1) and (3) gives:

$$\frac{d[HS^-]}{dt} = -k_1[HS^-](t)\frac{1}{2}X_b \tag{6}$$

Integration of Eq. (6) gives the parameter estimate $\hat{k}_1$:

$$\hat{k}_1 = 2\frac{\ln([HS^-](0)) - \ln([HS^{-1}](1))}{X_b} \tag{7}$$

After estimation of $\hat{k}_1$ and $\hat{K}_{i,1}$ the two remaining parameter estimates, $\hat{v}_{max}$ and $\hat{K}_{i,2}$ were found using a least-squares method (Linssen et al., 2023).

To judge the fit of the model predictions (y_i) to the dataset y_i^{data}, with $i = 1, 2, \cdots, N$, the root mean square error (RMSE) was calculated according to:

$$RMSE = \sqrt{\frac{\sum_{i=1}^{N}(y_i - y_i^{data})^2}{N}} \tag{8}$$

3.2. Model fit on new dataset

Model fits to the dataset are shown in Fig. 2 A-D, along with the measured HS^- values from each replicate. The measured anaerobic uptake is similar to that reported in Linssen et al. (2023). In all graphs, an initial fast sulfide uptake of about 0.20 mM is seen, regardless of pH. After this fast uptake, a slower uptake is seen until almost complete inhibition occurs due to accumulation of P_2. As the pH increases, the total amount of sulfide that is removed increases from approximately 0.20 mM at pH 7 to 0.35 mM at pH 10.

The model fit for Model 3 (Fig. 2 A-D) over the four different pH values was good, with an RMSE of 0.062. This result shows an improvement over the RMSE, calculated after refitting of the parameters, of 0.108 (Model 1) and 0.133 (Model 2) for the originally published models. Compared to the other two models, Model 3 is able to capture the initial sharp decline in $[HS^-]$ more accurately. For Model 3, k_1 was estimated at 0.009 ± 0.003 s^{-1} L mgN^{-1}, $K_{i,1}$ at 0.18 ± 0.04 mM, v_{max} at $2.10{\cdot}10^{-4}$ ± $0.58{\cdot}10^{-4}$ mM s^{-1} L mgN^{-1}. The model parameter $K_{i,2}$ showed a linear dependence on the process parameter pH, with the values of 0.010 ± 0.011 mM at pH 7.5, 0.042 ± 0.002 mM at pH 8, 0.054 ± 0.005 mM at pH 9 and 0.096 ± 0.022 mM at pH 10. Eq. (9) gives the empirical relationship between these two and its plot can be found in the supplementary information.

$$K_{i,2} = 0.031pH - 0.21 \tag{9}$$

3.3. Model fit on original dataset

Model 3 was tested on the original data from Linssen et al. (2023) and showed a good fit after re-estimation of k_1, estimated at 0.002 L s^{-1} mgN^{-1} (see supplementary information). The RMSE for the model fit on the original dataset is 0.036, which is lower than the value of 0.088 for Model 1 and comparable to the value of 0.041 for Model 2.

Re-estimation of k_1 is justified due to differences in biomass composition. The mixed cultures used by Linssen et al. (2023) and in this work both were dominated by *Thioalkalivibrio sulphidiphilus* (28 and 19 % relative abundance, respectively), *Alkalilimnicola ehrlichii* (16 and 24 %) and strains from the *Rhodobacteraceae* family (13 % and 4 %), in addition to containing *Izamaplasma sp.* (4 and 3 %). *Thioalkalivibrio sulphidiphilus, Alkalilimnicola ehrlichii*, and *Rhodobacteraceae* have been identified as sulfide oxidizing members of the core community in bio-desulfurization setups (Gupta et al., 2022). The remaining relative abundance of the culture used in Linssen et al. (2023) (39 %) and in this work (50 %) showed no overlap (see supplementary information).

Physiological differences between SOB species, such as size and membrane properties (Boden et al., 2017) can contribute to a different flux into the periplasmic space and lead to differences in r_1. Membrane properties such as thickness and composition influence its permeability to small solutes (Frallicciardi et al., 2022). Aside from permeability, specific membrane area and specific volume of the periplasmic space have been identified as relevant factors for transport into the periplasm (Nichols, 2017).

Previous research showed that the sulfide removal capacity per mgN was not constant with biomass concentration (Linssen et al., 2023). An experimental dataset (Linssen et al., 2023), carried out with 1 mM HS^- and 24 mgN L^{-1} biomass, was used to evaluate Model 3's ability to take this into account (Fig. 2E). Models 2 and 3, with RMSE values of 0.138 (Model 2) and 0.142 (Model 3), fit the data much better than Model 1, which predicted total HS^- depletion after 5 min and had an RMSE of 0.503. In contrast to Model 3, Model 1 assumed a fixed maximal sulfide removal per mgN, meaning that a higher biomass concentration leads to a higher removal. Models 2 and 3 assume that the maximal sulfide removal is independent of biomass concentration and that biomass concentration determines how long it takes to achieve this removal.

3.4. Mechanisms of anaerobic sulfide removal

The good fit of Model 3 supports the hypothesis that anaerobic sulfide removal is a multi-stage process. The polysulfides formed in the initial adsorption step r_1 can be stored in different forms. Linssen et al. (2023) have previously described a putative pathway in which the spontaneous cleavage of a long-chain organic polysulfide by HS^- (Eq. (10)) is followed by an enzymatic reaction of the cleaved polysulfide (Eq. (11)). After this cleavage, an even longer organic polysulfide is formed through an unknown mechanism (Eq. (12)):

$$RS_xS_yR + HS^- + H^+ \xrightarrow{spontanious} RS_xSH + RS_yH \tag{10}$$

$$RS_xSH \xrightarrow{enzymatic} RS_xS^+ + H^+ + 2e^- \tag{11}$$

$$RS_xS^+ + RS_yH \xrightarrow{?} RS_xSS_yR + H^+ \tag{12}$$

The fast reaction kinetics of r_1 fit the spontaneous polysulfide cleavage as described in Eq. (7). The fact that there is a critical concentration of P_1, represented by RS_xSH in Eq. (7) then points towards a chemical equilibrium being reached as described by Eq. (1). In this work, only $[HS^-]$ was measured and thus it is unclear how many steps there are after r_1. Therefore, r_2 represents the rate-limiting step in the sequence after r_1 but it is possible that P_2 represents a larger pool of reaction products as represented by Eqs. (11) and (12).

The dependence of $K_{i,2}$ on pH implies that P_2 is more stable when the pH increases. A similar trend was also observed by De Rink et al. who found more sulfide was anaerobically removed at a higher pH in a continuous bio-desulfurization setup (de Rink et al., 2021). The increased stability of P_2 at a higher pH fits with Eqs. (11) and (12), since in both reactions protons are formed.

Outlook

In this work, maximal anaerobic sulfide uptake was found to correlate with pH, with total uptake almost doubling between pH 7 and pH 10. In industrial desulfurization plants, the pH is not controlled at a fixed setpoint but rather is dependent on the H_2S/CO_2 ratio in the gas stream that is treated. Anaerobic sulfide removal partially explains the improved performance of the dual reactor system (de Rink et al., 2021). Therefore, pH is a parameter of more interest in future research in

process kinetics.

However, extending this model to industrial conditions requires further research. Under industrial operation, the HS^- concentrations are much higher than those used in this study. In a pilot reactor operated at 7, 15 and 25 mM HS^- a linear relationship was found between total sulfide and sulfide removal per mgN of biomass (de Rink et al., 2021). Thus future work must take place at these higher, industrially relevant, concentrations.

Secondly, the electron balance in the bacteria needs to be better understood. Eq. (11) states that two electrons are liberated per HS^- that is anaerobically removed. It is currently unknown where these electrons go, but it is clear that they are somehow stored in the bacteria (Linssen et al., 2024, 2023). Previous work has estimated that only 0.1 % of electron removal can be explained through the utilization of electron carriers such as ubiquinones and cytochromes (Linssen et al., 2023). This implies that other compounds play a role in the electron flow during sulfide removal. Characterization and quantification of charged (sulfur) species present in sulfide shuttling SOB is essential to fully understand the sulfide shuttling mechanisms.

4. Conclusion

A new model was developed and shown to perform better in terms of RMSE compared to prior models for anaerobic sulfide removal. The new model describes anaerobic sulfide removal using a fast chemical step followed by a slower biological step. The second step is dependent on pH, leading to a higher total removal with increasing pH (7.5–10). The two-stage model is supported by recent developments in research towards anaerobic sulfide removal and can be extended to industrial systems in future work.

CRediT authorship contribution statement

Joris Bergman: Writing – original draft, Visualization, Methodology, Formal analysis, Data curation. **Annemerel R. Mol:** Writing – review & editing, Supervision. **Annemiek ter Heijne:** Writing – review & editing, Supervision, Funding acquisition. **Karel J. Keesman:** Writing – review & editing, Supervision, Methodology, Funding acquisition. **Rikke Linssen:** Writing – original draft, Visualization, Project administration, Investigation, Formal analysis, Data curation, Conceptualization.

Declaration of competing interest

The authors declare that they have no known competing financial interests or personal relationships that could have appeared to influence the work reported in this paper.

Data availability

Data will be made available on request.

Acknowledgements

This work has been performed within the cooperation framework of Wetsus, the European Centre of Excellence for Sustainable Water Technology, Netherlands (wetsus.nl), and Wageningen University and Research, Netherlands (wur.nl). Wetsus is co-funded by the Dutch Ministry of Economic Affairs, the Ministry of Infrastructure and Environment, the European Union Regional Development Fund, the Northern Netherlands Provinces, and the Province of Fryslân. This work is co-financed by the Dutch Research Council (NWO), Vidi project 17516, and by Paqell B.V. The authors thank Dr. Margo Elzinga for proof reading the article and Aaron van der Wel, BSc for helping to collect the data.

Appendix A. Supplementary data

Supplementary data to this article can be found online at https://doi.org/10.1016/j.biortech.2024.131064.

References

Boden, R., Scott, K.M., Williams, J., Russel, S., Antonen, K., Rae, A.W., Hutt, L.P., 2017. An evaluation of Thiomicrospira, Hydrogenovibrio and Thioalkalimicrobium: reclassification of four species of Thiomicrospira to each Thiomicrorhabdus gen. nov. and Hydrogenovibrio, and reclassification of all four species of Thioalkalimicrobium to Thiomicrospira. Int. J. Syst. Evol. Microbiol. https://doi.org/10.1099/ijsem.0.001855.

de Rink, R., Gupta, S., Piccioli de Carolis, F., Liu, D., ter Heijne, A., Klok, J.B.M., Buisman, C.J.N., 2021. Effect of process conditions on the performance of a dual-reactor biodesulfurization process. J. Environ. Chem. Eng. 9, 106450 https://doi.org/10.1016/j.jece.2021.106450.

De Smit, S.M., de Leeuw, K.D., Buisman, C.J., Strik, D.P., 2019. Continuous n-valerate formation from propionate and methanol in an anaerobic chain elongation open-culture bioreactor. Biotechnol. Biofuels 12, 1–16.

Feilberg, A., Hansen, M.J., Liu, D., Nyord, T., 2017. Contribution of livestock H2S to total sulfur emissions in a region with intensive animal production. Nat. Commun. 8, 1069. https://doi.org/10.1038/s41467-017-01016-2.

Frallicciardi, J., Melcr, J., Siginou, P., Marrink, S.J., Poolman, B., 2022. Membrane thickness, lipid phase and sterol type are determining factors in the permeability of membranes to small solutes. Nat. Commun. 13, 1605. https://doi.org/10.1038/s41467-022-29272-x.

Gupta, S., Plugge, C.M., Klok, J.B., Muyzer, G., 2022. Comparative analysis of microbial communities from different full-scale haloalkaline biodesulfurization systems. Appl. Microbiol. Biotechnol. 106, 1759–1776.

Holmberg, A., Ranta, J., 1982. Procedures for parameter and state estimation of microbial growth process models. Automatica 18, 181–193.

Janssen, A.J., Lens, P.N., Stams, A.J., Plugge, C.M., Sorokin, D.Y., Muyzer, G., Dijkman, H., Van Zessen, E., Luimes, P., Buisman, C.J., 2009. Application of bacteria involved in the biological sulfur cycle for paper mill effluent purification. Sci. Total Environ. 407, 1333–1343.

Kiragosyan, K., Picard, M., Sorokin, D.Y., Dijkstra, J., Klok, J.B., Roman, P., Janssen, A.J., 2020. Effect of dimethyl disulfide on the sulfur formation and microbial community composition during the biological H2S removal from sour gas streams. J. Hazard. Mater. 386, 121916.

Klok, J.B., 2015. Modeling studies of biological gas desulfurization under haloalkaline conditions (Doctoral). Wageningen University, Wageningen.

Linssen, R., de Smit, S., Röhring (neé Neubert), K., Harnisch, F., ter Heijne, A., 2024. Revealing cellular (poly)sulphide storage in electrochemically active sulphide oxidising bacteria using rotating disc electrodes. Bioelectrochemistry 108710. doi: 10.1016/j.bioelechem.2024.108710.

Linssen, R., Slinkert, T., Buisman, C.J.N., Klok, J.B.M., ter Heijne, A., 2023. Anaerobic sulphide removal by haloalkaline sulphide oxidising bacteria. Bioresour. Technol. 369, 128435 https://doi.org/10.1016/j.biortech.2022.128435.

Muloiwa, M., Nyende-Byakika, S., Dinka, M., 2020. Comparison of unstructured kinetic bacterial growth models. S. Afr. J. Chem. Eng. 33, 141–150.

Nichols, W.W., 2017. Modeling the kinetics of the permeation of antibacterial agents into growing bacteria and its interplay with efflux. Antimicrob. Agents Chemother. 61, 10–1128.

Singh, A.K., Chandra, R., 2019. Pollutants released from the pulp paper industry: Aquatic toxicity and their health hazards. Aquat. Toxicol. 211, 202–216.